ACS APPLIED MATERIALS & INTERFACES

Research Article

www.acsami.org

High-Performance GaAs Nanowire Solar Cells for Flexible and Transparent Photovoltaics

Ning Han,[†,‡] Zai-xing Yang,[‡,§,∥] Fengyun Wang,[⊥] Guofa Dong,[‡,∥] SenPo Yip,[‡,§,∥] Xiaoguang Liang,[‡] Tak Fu Hung,[‡] Yunfa Chen,[*,†] and Johnny C. Ho[*,‡,§,∥]

[†]State Key Laboratory of Multiphase Complex Systems, Institute of Process Engineering, Chinese Academy of Sciences, Beijing, 100190, P.R. China

[‡]Department of Physics and Materials Science and [§]State Key Laboratory of Millimeter Waves, City University of Hong Kong, Kowloon Tong, Hong Kong

[∥]Shenzhen Research Institute, City University of Hong Kong, Shenzhen, 518057, P.R. China

[⊥]Cultivation Base for State Key Laboratory, Qingdao University, Qingdao, 266071, P.R. China

Supporting Information

ABSTRACT: Among many available photovoltaic technologies at present, gallium arsenide (GaAs) is one of the recognized leaders for performance and reliability; however, it is still a great challenge to achieve cost-effective GaAs solar cells for smart systems such as transparent and flexible photovoltaics. In this study, highly crystalline long GaAs nanowires (NWs) with minimal crystal defects are synthesized economically by chemical vapor deposition and configured into novel Schottky photovoltaic structures by simply using asymmetric Au−Al contacts. Without any doping profiles such as p−n junction and complicated coaxial junction structures, the single NW Schottky device shows a record high apparent energy conversion efficiency of 16% under air mass 1.5 global illumination by normalizing to the projection area of the NW. The corresponding photovoltaic output can be further enhanced by connecting individual cells in series and in parallel as well as by fabricating NW array solar cells via contact printing showing an overall efficiency of 1.6%. Importantly, these Schottky cells can be easily integrated on the glass and plastic substrates for transparent and flexible photovoltaics, which explicitly demonstrate the outstanding versatility and promising perspective of these GaAs NW Schottky photovoltaics for next-generation smart solar energy harvesting devices.

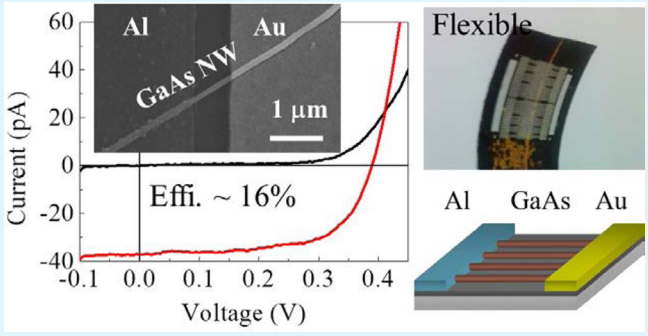

KEYWORDS: *GaAs nanowires, Schottky contact, photovoltaics, output reinforcement, transparent and flexible solar cells*

INTRODUCTION

Because of their excellent light-to-electricity conversion efficiency and extraordinary radiation hardness, gallium arsenide (GaAs) photovoltaics have been long used for space applications; however, the high production cost of crystalline GaAs thin films and their complex junctions greatly limits their adoption in terrestrial and domestic utilizations.[1,2] Although the recent advent of nanotechnology can significantly reduce the material consumption of GaAs in various nanostructures, the epitaxial growth of two-dimensional nanoscale thin films or one-dimensional nanowires (NWs) on costly crystalline substrates as well as the high-temperature enabled junction formation still hinder the domestic usage of GaAs-based solar cells. Therefore, it is highly desirable to synthesize GaAs photovoltaic nanomaterials on noncrystalline substrates and to form electron/hole separating barriers in a moderate processing condition; this way, these obtained lightweight terrestrial solar panels can not only substantially minimize the transportation cost but also facilitate the realization of smart solar cells such as integrating flexible cells into clothing and transparent windows.[2−6]

At the same time, GaAs NWs are lately reported to have the outstanding energy conversion efficiency of 9−11%,[7,8] higher than those records of other flexible counterparts such as organic photovoltaics.[9] In particular, the vertical GaAs NW with radial p-i-n junction is demonstrated with the outstanding apparent efficiency of 40%, beyond the Shockley-Queisser limit due to the far larger light absorption area than the projected cross-sectional area of NWs,[10] where it clearly indicates the potential of GaAs NWs for applications in smart photovoltaics. With the aim to further reduce the material and processing cost for large-scale deployments, as a proof-of-concept, we synthesize GaAs NWs on noncrystalline SiO_2/Si substrates and fabricate facile Schottky barrier structured NW solar cells employing enhanced

Received: July 19, 2015
Accepted: August 18, 2015
Published: August 18, 2015

DOI: 10.1021/acsami.5b06452
ACS Appl. Mater. Interfaces 2015, 7, 20454−20459

Au−Al asymmetric contacts, with the highest single NW photovoltaic apparent efficiency of 16% under air mass (AM) 1.5G illumination. Importantly, these attained NWs can also be contact-printed into parallel arrays on glass and polyimide substrates to achieve efficient transparent and flexible solar cells, respectively, which illustrate promising perspectives of GaAs NWs for future smart solar devices.

EXPERIMENTAL SECTION

In this work, the GaAs NWs are synthesized in a solid-source chemical vapor deposition (SSCVD) system utilizing a two-step process with GaAs powders as the starting material (0.6−1.5 g, 99.999% purity), and thermally deposited Au films (12 nm) as the catalyst as reported previously.[11,12] The Au catalyst film (thermally deposited onto 50 nm SiO_2/Si, with the dimension of 5 cm long and 1 cm wide) is placed in the downstream zone of a two-zone furnace, annealed into nanoparticles at 800 °C for 10 min, and then cooled down to 650 °C under the pressure of ∼1 Torr in H_2 atmosphere (99.99% purity, flow at 100 standard cubic centimeters per minute, sccm). Then the GaAs powders are held in a boron nitride crucible located in the upstream zone, which is heated at 800−900 °C. The evaporated precursors are transported by H_2 flow to the Au catalyst. After the 5 min nucleation step at 650 °C, the growth temperature is lowered to 600 °C for a growth duration of 60 min. The system is finally cooled down to room temperature in H_2 atmosphere and the NWs are harvested for further characterization and solar device fabrication. The morphology of NWs is observed by a scanning electron microscope (SEM, FEI/Philips XL30) and transmission electron microscope (TEM, Philips CM20). The corresponding crystal structure is analyzed by using X-ray diffraction (XRD) recorded on a Philips powder diffractometer (40 kV, 30 mA) with the Cu Kα radiation (λ = 0.154 nm) and selective area electron diffraction pattern (SAED) imaged with TEM (CM20).

The obtained GaAs NWs are then dispersed in anhydrous ethanol by sonication and drop-casted onto the SiO_2/Si (50 nm thermally grown oxide) substrate. The first Schottky electrode layer of single NW solar cell devices are defined by ultraviolet photolithography (SUSS MA6) using LOR 3A lift-off resist and AZ5206 photoresist, and metal electrodes are obtained by thermal evaporation and subsequent lift-off process. The second asymmetric electrode layer is obtained by a repeated procedure of photolithography, metal deposition, and liftoff. The GaAs NW arrays are fabricated by contact printing.[13] In brief, the device substrate (SiO_2/Si, 50 nm thick thermally grown oxide) is initially modified by mild O_2 plasma and polylysine (0.5 v/v % aqueous solution). Then it is blow-dried with N_2. Afterward, the NW donor substrate is flipped and slid against the surface of the device substrate at a velocity of 10 mm/min under a pressure of 50 g/cm^2. It is noted that the NW printing on glass is performed with the same condition as the one on silicon substrates. On the other hand, since the plastic substrate has a relatively rougher surface, the nanowire printing requires a higher pressure of 100 g/cm^2 there. The subsequent asymmetric metal electrode layers of NW array solar cells are defined in the same way as those of single NW devices. The solar cell performance is measured using a semiconductor analyzer (Agilent 4155C) and a standard probe station under illumination of a solar simulator (Newport 96000).

RESULTS AND DISCUSSION

The GaAs NWs prepared by the two-step growth method are highly dense on the noncrystalline SiO_2/Si substrate with length >20 μm and exhibit purely single-crystalline cubic zinc blende phase as demonstrated in scanning electron microscope (SEM) and X-ray diffraction (XRD) analysis in Figure 1a. Specifically, one representative individual NW is imaged by transmission electron microscope (TEM) with the typical diameter of ∼90 nm as shown in Figure 1b and growth orientation of ⟨111⟩ as determined from selected area electron diffraction (SAED), which is the most preferential growth orientation as reported in our previous study.[11] The Au catalytic tip is clearly observed on top of the NW, inferring the vapor−liquid−solid (VLS) growth mechanism of NWs, with details reported in previous studies, where the long NWs with excellent crystallinity are attributed to the relatively higher Ga supersaturation in the Au catalytic seeds obtained by the high-temperature nucleation step in the two-step growth method.[11,14] It should be noted that when more than 1 g of GaAs source powder is used, or higher source temperature than 900 °C is adopted, the obtained NWs will have serious surface-coating problems as illustrated in Figure S1 of the Supporting Information. This overcoating is always due to the competition between vapor−solid (VS) and VLS growth as more than required precursors are practically provided during the CVD process.[12,15] In contrast, the GaAs NWs prepared by a suitable amount of source powder (i.e., 0.7 g) at a moderate source temperature (i.e., 860 °C) would have the minimized coating issue. Importantly, these coating layers are found to possess abundant surface trap states deteriorating the electrical properties of GaAs NWs, which are experimentally shown to have fatal effects on the NW photovoltaic performance in our earlier studies as well as in the literature.[7,16,17] Therefore, only the smooth NWs are adopted for the photovoltaic applications in the following section, with SEM image and corresponding NW diameter statistics shown in Figure S1 of the Supporting Information.

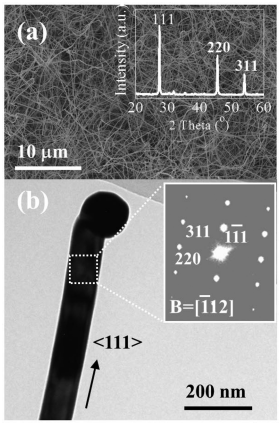

Figure 1. Morphology and structural characterizations of the grown GaAs NWs. (a) SEM image and corresponding XRD pattern (inset); (b) TEM image of one representative NW grown along the ⟨111⟩ direction as identified by the SAED pattern in the inset.

To achieve low-temperature solar cell fabrication, Schottky barrier photovoltaic structure, rather than the high-temperature p-n junction formation, is implemented here by employing asymmetric metal electrodes with one electrode having relatively higher work function (W) while the other has lower W. Au is adopted as the typical high W electrode (∼5.4 eV) while the lower W metals, such as Ni (∼5.1 eV), Cr (∼4.5 eV), and Al (∼4.2 eV), are utilized.[18,19] The high W metal would constitute a Schottky contact to photoelectrons of the GaAs NW, while the low W metal would yield a Schottky contact to the photogenerated holes. After the cell fabrication, Figure 2a gives the open-circuit voltage (V_{OC}) obtained in the single NW devices with various work function difference ($W_{High} - W_{Low}$) of the asymmetric electrodes. On the basis of the statistics of 20 different single NW devices, it is obvious that the Au−Ni electrode pair has the smallest work function difference (∼0.3

DOI: 10.1021/acsami.5b06452
ACS Appl. Mater. Interfaces 2015, 7, 20454−20459

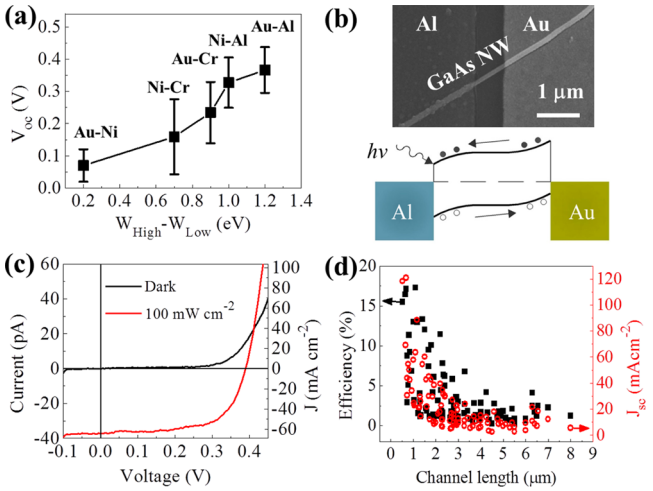

Figure 2. Fundamentals of single NW Schottky barrier solar cells. (a) Dependence of the open-circuit voltage (V_{OC}) on the work function difference ($W_{High} - W_{Low}$) of the two asymmetric metal electrodes (statistics of 20 cells in each structure), (b) SEM image and corresponding band diagram of the single GaAs NW Schottky barrier solar cell suing Au−Al electrodes, (c) $I-V$ curves of the solar cell in (b), and (d) dependence of the efficiency and short-circuit current density (J_{SC}) on the channel length of the single NW solar cells (collected with 100 cells in the Au−Al structure).

eV) and hence yields the smallest V_{OC} (<0.1 V). Similarly, since the Au−Al electrode pair has the largest work function difference (~1.0 eV) among all the electrodes explored in this work, the highest V_{OC} (~0.36 V) is expected. Notably, it is confirmed that the resulting V_{OC} scales with the work function difference employed in the asymmetric electrodes accordingly. Also, these Schottky barrier NW solar cells are highly versatile by simply using asymmetric electrodes, without any doping profiling and complicated device structure. Although the V_{OC} obtained is a bit smaller than the work function difference of the metal electrodes involved, this discrepancy can be probably attributed to the slightly different surface Fermi level pinning for various NW/metal interfaces, depending on the choice of metal, metal thickness, conductance, and others.[20−22] Specifically, the SEM image, energy band diagram, and current−voltage ($I-V$) characteristics of one representative NW devices with Au−Al asymmetric electrodes are depicted in Figure 2b,c. The details of other devices, including Au−Ni, Au−Cr, Ni−Cr, and Ni−Al electrodes, are shown in Figure S2 of the Supporting Information. It is clear that this Au−Al device yields a V_{OC} of 0.39 V, an apparent short-circuit current (J_{SC}) of 67 mA cm^{-2}, and a fill factor (FF) of 0.61 under AM 1.5 G illumination, which corresponds to the record high apparent energy conversion efficiency of 16% based on the active horizontal NW channel length of 0.65 μm and diameter of ~85 nm, even higher than those complicated p-i-n NW structures as listed in Table 1. Considering the noncrystalline growth substrate and facile formation of Schottky barrier, this kind of GaAs NW solar cells is demonstrated with great promise for low-cost and high-efficiency photovoltaics.[23]

To shed light on probable reasons for achieving this superior efficiency, further insights into the photo-electricity conversion process of NWs is necessary. It is well understood that there are two key successive steps in the solar energy harvesting by photovoltaics. The first step is the effective photon absorption by active materials followed by the second step of the instantaneous separation and the collection of photoinduced electron/holes.[24,25] It is both experimentally and theoretically proved that one-dimensional NWs can have better light absorption characteristics than their bulk counterparts, and an apparent efficiency of 40% beyond the Shockley-Queisser limit has been accomplished by vertical-structured GaAs photovoltaics.[10,26−28] It is therefore the horizontal NW channel configured in this work that would also possess higher light absorption characteristics than the one of thin films even though the NW absorption thickness is lower, which show the low-cost advantages of NW based photovoltaics as well as photodetectors by the resonant light absorption effect. On the other hand, the grown GaAs NWs are single-crystalline with minimal crystal defects observed due to the relatively higher Ga supersaturation in Au catalytic seeds during the growth process as reported in our previous study.[11,14] Also, since no dopant is utilized here, there would not be any impurity centers for the electron/holes recombination. All these minimized defects and scattering centers would then contribute to the longer minority lifetime which is favorable for efficient photoinduced electron/hole separation and collection. From the literature, one can find the electron mobility (μ) of GaAs NW around 4000 cm^2 V^{-1} s^{-1} and electron lifetime (τ) on the order of 10^2 ps,[29−33] resulting in an electron diffusion length around 1 μm as estimated by the equation $(\mu\tau kT/e)^{1/2}$ (where kT/e is constant), which is in good agreement with the electron beam induced current (EBIC) and Kelvin probe force microscopy (KPFM) measurements.[34,35] All these are completely consistent with our results presented in Figure 2d in which the photovoltaic performance statistics (based on 100 single NW devices) explicitly show that the high efficiency and large J_{SC} are only obtained for the channel length <1 μm. The channel length dependent V_{OC} and FF are given in Figure S3 of the Supporting Information. These findings are extremely

Table 1. Comparison of GaAs NW Schottky Solar Cells with Other III−V Photovoltaics Reported in the Literature

material	method	substrate	junction	structure	efficiency	ref
GaAs NW	SSCVD	noncrystalline	Schottky contact	horizontal	16%[c]	this work
GaAsP NW	MBE[a]	Si(111)	radial p-i-n	horizontal	10.2%[c]	7
GaAs NW	MBE	GaAs(111)	radial p-i-n	horizontal	4.5%[c]	44
GaAs NW	MBE	Si(111)	radial p-i-n	vertical	40%[c]	10
GaAs NW array	MOCVD[b]	GaAs(111)	radial p-n, InGaP cap	vertical	6.63%	17
GaAs NW array	etched	GaAs(100)	GaAs/PEDOT:PSS	vertical	9.2%	8
InP NW array	MBE	p-InP	axial p-i-n	vertical	13.8%	45
GaAs sheets	MOCVD	GaAs(100)	planar p-n	vertical	14.5%	46

[a]Molecular beam epitaxy. [b]Metal organic chemical vapor deposition. [c]Apparent efficiency normalized to the projection area of the single NW, i.e, efficiency = $[(V_{OC} \times I_{SC} \times FF)/(100\ mW/cm^2 \times diameter \times active\ length)] \times 100\%$.

DOI: 10.1021/acsami.5b06452
ACS Appl. Mater. Interfaces 2015, 7, 20454−20459

beneficial for the design of solar cell structure to achieve the highest efficiency with the optimized active material area matching the carrier diffusion length.

It is noticeable that although the obtained efficiency is high, the single NW solar cells have relatively low output voltage and current. With the purpose of being practical for wide application domains, we have adopted two strategies to enhance and reinforce the output. One approach is to connect individual single NW solar cells while the other one is to fabricate solar cells based on NW arrays. Figure 3 demonstrates

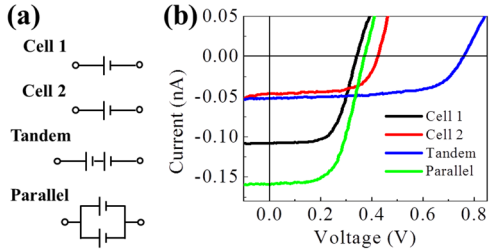

Figure 3. Performance of single NW solar cells connected in tandem and parallel configuration. (a) Equivalent circuit diagrams and (b) *I*–*V* curves of two individual cells connected in tandem and in parallel (cell 1 shown in Figure S3 of the Supporting Information and cell 2 shown in Figure 2).

clearly the proof-of-concept by connecting two individual single NW solar cells in tandem (in series) to reinforce the voltage and in parallel to enhance the current.[36] At the same time, the GaAs NW parallel arrays are as well fabricated by contact printing,[13,37] and the optimized Au–Al asymmetric electrodes are deposited to achieve the Schottky solar cells as depicted in Figure 4. It is obvious that the printed NW density is ~1.5

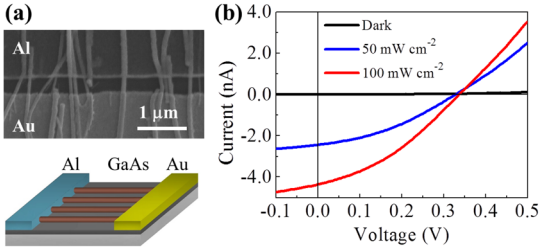

Figure 4. Performance of the GaAs NW array Schottky solar cell fabricated on SiO_2/Si substrate. (a) SEM image and device schematic and (b) *I*–*V* curves of the GaAs NW array solar cell fabricated by contact printing with optimized Au–Al asymmetric Schottky electrodes.

NW/μm, accounting for a total of 300 NWs in the 200 μm wide device (Figure 4a). As compared to that of the single NW device, the output performance of this NW array cell is significantly improved (Figure 4b), with the V_{OC} of 0.34 V, I_{SC} of 4.36 nA, FF of 0.36, and estimation of conversion efficiency of ~11% by considering the total absorption (projected) area of the NWs under AM 1.5 G illumination. Notably, since a large part of the channel area is not covered with the GaAs NWs, this will discount the total efficiency to ~1.6% by considering the overall channel area. This efficiency is in good accordance with the single NW one if one estimates ~10× absorption area than the NW projected area, which can be further improved by increasing the absorption thickness (i.e., NW diameter).[38] In any case, the GaAs NW array Schottky solar cell shows the respectable and uniform photovoltaic performance, with higher efficiency achievable by fabricating higher density NW arrays with optimized NW contact printing or other NW aligning technologies such as flow-assisted method and electrophoresis alignment, etc.[23,39,40]

Once the two above-mentioned approaches are found successfully to boost up the output performance of Schottky solar cells, similar cell structures are built on nonconventional substrates for smart photovoltaics such as fabricating on glass for transparent solar cells (Figure 5) as well as on polyimide for

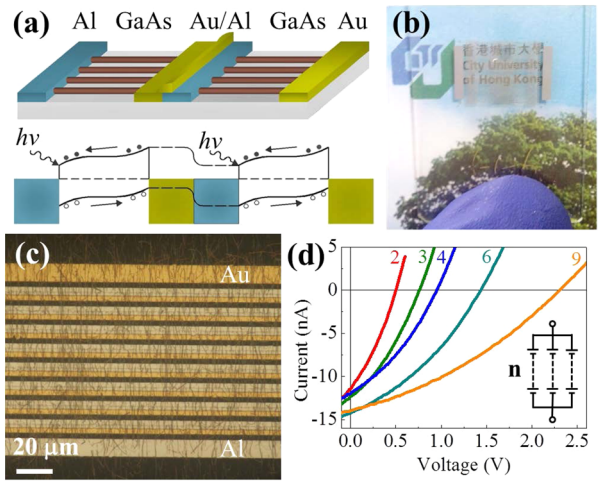

Figure 5. Transparent GaAs NW array Schottky solar cells constructed on glass. (a) Device schematic and corresponding band diagram, (b) photograph, (c) microscope image, and (d) *I*–*V* curves of the transparent solar cell (2, 3, 4, 6, and 9 cells connected in tandem along with 3 such devices configured in parallel readily by lithography).

flexible photovoltaic cells (Figure 6). Figure 5a depicts the device schematic and band alignment of the GaAs NW array Schottky solar cell connected in tandem readily by conventional lithography.[36] Figure 5b,c gives the picture and microscopic

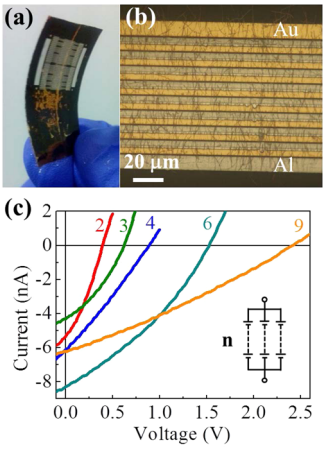

Figure 6. Flexible GaAs NW array Schottky solar cells fabricated on polyimide. (a) Photograph, (b) microscope image, and (c) *I*–*V* curves of the flexible solar cell (2, 3, 4, 6, and 9 cells connected in tandem along with 3 such devices configured in parallel readily by lithography).

DOI: 10.1021/acsami.5b06452
ACS Appl. Mater. Interfaces 2015, 7, 20454–20459

image of one typical transparent solar cell constructed on glass, with the output curves of 2, 3, 4, 6, and 9 cells connected in tandem along with 3 such devices configured in parallel as illustrated in Figure 5d. It is apparent that the corresponding photovoltaic output can be reinforced effectively by the tandem configuration with the output voltage of ~2.4 V and output current of ~15 nA (9 tandem and 3 parallel cells connection). Importantly, the output voltage is scaled linearly with the number of cells connected in series, indicating the uniformity of NWs printed in the device channel suitable for large-scale applications. Also, the optical transparency of these cells fabricated on glass is also assessed and confirmed by the microscope imaging in the transmission mode (Figure S4 of the Supporting Information), suggesting the potential usage of these Schottky cells for smart windows.[41−43] Similarly, the GaAs NW array Schottky solar cells are as well fabricated onto the 100-μm-thick polyimide substrate, with the picture and microscope image shown in Figure 6a,b. As given in Figure 6c, the output voltage is again ~2.4 V (9 tandem and 3 parallel cells connection) while the output current is ~6.5 nA, slightly lower than the ones fabricated on glass due to the inefficient NW printing on a nonsmooth surface (i.e., polyimide).[13] It is noted that, in these proof-of-concept smart solar cell examples, the efficiency is relatively lower than that of single NW devices since the V_{OC} and FF are only ~0.27 V and ~0.35 per device probably due to the somewhat higher contact resistance which will be optimized further. Also, the NW density can be further enhanced by improved contact printing or other NW alignment techniques to obtain higher output current. Nevertheless, these transparent and flexible Schottky solar cells, based on high-performance GaAs NWs synthesized cost-effectively on non-crystalline substrates, are demonstrated with the great promise for smart photovoltaics.

CONCLUSIONS

High-density GaAs nanowires (NWs) with minimal crystal defects and length >20 μm are prepared in large scale on noncrystalline SiO_2/Si substrates by a facile solid-source chemical vapor deposition method. The obtained NWs exhibit superior apparent sunlight-to-electricity conversion efficiency up to ~16% in a moderate Schottky barrier structured photovoltaic cell, attributing to the efficient light absorption and enhanced electron/hole diffusion length due to the excellent crystal quality attained by the two-step growth process. Importantly, these NW solar cells can be further connected in parallel arrays in tandem and in parallel to reinforce their photovoltaic output, integrating onto glass and plastic substrates for transparent and flexible solar cells, respectively. All these results have demonstrated the outstanding versatility and promising perspective of GaAs NW Schottky solar cells for next-generation smart solar energy harvesting devices.

ASSOCIATED CONTENT

Supporting Information

SEM images and diameter distribution, IV curves of PVs, channel length independent V_{oc} and FF, and transmittance microscope image of transparent solar cell. The Supporting Information is available free of charge on the ACS Publications website at DOI: 10.1021/acsami.5b06452.

AUTHOR INFORMATION

Corresponding Authors

*E-mail: johnnyho@cityu.edu.hk (J.C.H.).
*E-mail: yfchen@ipe.ac.cn (Y.C.).

Notes

The authors declare no competing financial interest.

ACKNOWLEDGMENTS

This research was financially supported by the Early Career Scheme of the Research Grants Council of Hong Kong SAR, China (CityU 139413), the National Natural Science Foundation of China (Grants 51202205 and 51402160), the State Key Laboratory of Multiphase Complex Systems (MPCS-2014-C-01 and MPCS-2015-A-04), the Applied Basic Research Foundation of Qingdao City (Grant 14-2-4-45-jch), and the Science Technology and Innovation Committee of Shenzhen Municipality (Grant JCYJ20140419115507588), and was also supported by a grant from the Shenzhen Research Institute, City University of Hong Kong.

REFERENCES

(1) Butler, D. Thin Films: Ready for Their Close-Up? *Nature* **2008**, *454*, 558−559.
(2) Schubert, M. B.; Werner, J. H. Flexible Solar Cells for Clothing. *Mater. Today* **2006**, *9*, 42−50.
(3) LaPierre, R. R.; Chia, A. C. E.; Gibson, S. J.; Haapamaki, C. M.; Boulanger, J.; Yee, R.; Kuyanov, P.; Zhang, J.; Tajik, N.; Jewell, N.; Rahman, K. M. A. III-V Nanowire Photovoltaics: Review of Design for High Efficiency. *Phys. Status Solidi RRL* **2013**, *7*, 815−830.
(4) Dhaka, V.; Haggren, T.; Jussila, H.; Jiang, H.; Kauppinen, E.; Huhtio, T.; Sopanen, M.; Lipsanen, H. High Quality GaAs Nanowires Grown on Glass Substrates. *Nano Lett.* **2012**, *12*, 1912−1918.
(5) Lunt, R. R.; Bulovic, V. Transparent, near-Infrared Organic Photovoltaic Solar Cells for Window and Energy-Scavenging Applications. *Appl. Phys. Lett.* **2011**, *98*, 113305.
(6) Yu, R.; Lin, Q. F.; Leung, S. F.; Fan, Z. Y. Nanomaterials and Nanostructures for Efficient Light Absorption and Photovoltaics. *Nano Energy* **2012**, *1*, 57−72.
(7) Holm, J. V.; Jorgensen, H. I.; Krogstrup, P.; Nygard, J.; Liu, H. Y.; Aagesen, M. Surface-Passivated GaAsP Single-Nanowire Solar Cells Exceeding 10% Efficiency Grown on Silicon. *Nat. Commun.* **2013**, *4*, 1498.
(8) Chao, J. J.; Shiu, S. C.; Lin, C. F. Gaas Nanowire/Poly(3,4-Ethylenedioxythiophene):Poly(Styrenesulfonate) Hybrid Solar Cells with Incorporating Electron Blocking Poly(3-Hexylthiophene) Layer. *Sol. Energy Mater. Sol. Cells* **2012**, *105*, 40−45.
(9) Cao, W. R.; Xue, J. G. Recent Progress in Organic Photovoltaics: Device Architecture and Optical Design. *Energy Environ. Sci.* **2014**, *7*, 2123−2144.
(10) Krogstrup, P.; Jorgensen, H. I.; Heiss, M.; Demichel, O.; Holm, J. V.; Aagesen, M.; Nygard, J.; Fontcuberta i Morral, A. Single-Nanowire Solar Cells Beyond the Shockley-Queisser Limit. *Nat. Photonics* **2013**, *7*, 306−310.
(11) Han, N.; Hou, J. J.; Wang, F. Y.; Yip, S.; Yen, Y. T.; Yang, Z. X.; Dong, G. F.; Hung, T.; Chueh, Y. L.; Ho, J. C. GaAs Nanowires: From Manipulation of Defect Formation to Controllable Electronic Transport Properties. *ACS Nano* **2013**, *7*, 9138−9146.
(12) Han, N.; Wang, F. Y.; Hui, A. T.; Hou, J. J.; Shan, G. C.; Xiu, F.; Hung, T. F.; Ho, J. C. Facile Synthesis and Growth Mechanism of Ni-Catalyzed GaAs Nanowires on Non-Crystalline Substrates. *Nanotechnology* **2011**, *22*, 285607.
(13) Fan, Z. Y.; Ho, J. C.; Takahashi, T.; Yerushalmi, R.; Takei, K.; Ford, A. C.; Chueh, Y. L.; Javey, A. Toward the Development of Printable Nanowire Electronics and Sensors. *Adv. Mater.* **2009**, *21*, 3730−3743.

DOI: 10.1021/acsami.5b06452
ACS Appl. Mater. Interfaces 2015, 7, 20454−20459

(14) O'Regan, C.; Biswas, S.; O'Kelly, C.; Jung, S. J.; Boland, J. J.; Petkov, N.; Holmes, J. D. Engineering the Growth of Germanium Nanowires by Tuning the Supersaturation of Au/Ge Binary Alloy Catalysts. *Chem. Mater.* **2013**, *25*, 3096−3104.
(15) Perea, D. E.; Hemesath, E. R.; Schwalbach, E. J.; Lensch-Falk, J. L.; Voorhees, P. W.; Lauhon, L. J. Direct Measurement of Dopant Distribution in an Individual Vapour-Liquid-Solid Nanowire. *Nat. Nanotechnol.* **2009**, *4*, 315−319.
(16) Tajik, N.; Peng, Z.; Kuyanov, P.; LaPierre, R. Sulfur Passivation and Contact Methods for Gaas Nanowire Solar Cells. *Nanotechnology* **2011**, *22*, 225402.
(17) Mariani, G.; Scofield, A. C.; Hung, C. H.; Huffaker, D. L. GaAs Nanopillar-Array Solar Cells Employing in Situ Surface Passivation. *Nat. Commun.* **2013**, *4*, 1497.
(18) Lide, D. R. *CRC Handbook of Chemistry and Physics*; CRC Press: Boca Raton, FL, 2010.
(19) Han, N.; Wang, F.; Yip, S.; Hou, J. J.; Xiu, F.; Shi, X.; Hui, A. T.; Hung, T.; Ho, J. C. GaAs Nanowire Schottky Barrier Photovoltaics Utilizing Au-Ga Alloy Catalytic Tips. *Appl. Phys. Lett.* **2012**, *101*, 013105.
(20) del Alamo, J. A. Nanometre-Scale Electronics with III-V Compound Semiconductors. *Nature* **2011**, *479*, 317−323.
(21) Han, N.; Wang, F. Y.; Hou, J. J.; Yip, S. P.; Lin, H.; Xiu, F.; Fang, M.; Yang, Z. X.; Shi, X. L.; Dong, G. F.; Hung, T. F.; Ho, J. C. Tunable Electronic Transport Properties of Metal-Cluster-Decorated III-V Nanowire Transistors. *Adv. Mater.* **2013**, *25*, 4445−4451.
(22) Newman, N.; Spicer, W.; Kendelewicz, T.; Lindau, I. On the Fermi Level Pinning Behavior of Metal/III−V Semiconductor Interfaces. *J. Vac. Sci. Technol., B: Microelectron. Process. Phenom.* **1986**, *4*, 931−938.
(23) Long, Y. Z.; Yu, M.; Sun, B.; Gu, C. Z.; Fan, Z. Y. Recent Advances in Large-Scale Assembly of Semiconducting Inorganic Nanowires and Nanofibers for Electronics, Sensors and Photovoltaics. *Chem. Soc. Rev.* **2012**, *41*, 4560−4580.
(24) Meng, S.; Ren, J.; Kaxiras, E. Natural Dyes Adsorbed on TiO_2 Nanowire for Photovoltaic Applications: Enhanced Light Absorption and Ultrafast Electron Injection. *Nano Lett.* **2008**, *8*, 3266−3272.
(25) Wang, Z. S.; Cui, Y.; Hara, K.; Dan-Oh, Y.; Kasada, C.; Shinpo, A. A High-Light-Harvesting-Efficiency Coumarin Dye for Stable Dye-Sensitized Solar Cells. *Adv. Mater.* **2007**, *19*, 1138−1141.
(26) Cao, L. Y.; White, J. S.; Park, J. S.; Schuller, J. A.; Clemens, B. M.; Brongersma, M. L. Engineering Light Absorption in Semiconductor Nanowire Devices. *Nat. Mater.* **2009**, *8*, 643−647.
(27) Kempa, T. J.; Cahoon, J. F.; Kim, S. K.; Day, R. W.; Bell, D. C.; Park, H. G.; Lieber, C. M. Coaxial Multishell Nanowires with High-Quality Electronic Interfaces and Tunable Optical Cavities for Ultrathin Photovoltaics. *Proc. Natl. Acad. Sci. U. S. A.* **2012**, *109*, 1407−1412.
(28) Li, X.; Yaohui, Z.; Wang, C. Broadband Enhancement of Coaxial Heterogeneous Gallium Arsenide Single-Nanowire Solar Cells. *Prog. Photovoltaics* **2015**, *23*, 628−636.
(29) Fortuna, S. A.; Li, X. L. GaAs Mesfet with a High-Mobility Self-Assembled Planar Nanowire Channel. *IEEE Electron Device Lett.* **2009**, *30*, 593−595.
(30) Spirkoska, D.; Arbiol, J.; Gustafsson, A.; Conesa-Boj, S.; Glas, F.; Zardo, I.; Heigoldt, M.; Gass, M. H.; Bleloch, A. L.; Estrade, S.; Kaniber, M.; Rossler, J.; Peiro, F.; Morante, J. R.; Abstreiter, G.; Samuelson, L.; Fontcuberta i Morral, A. Structural and Optical Properties of High Quality Zinc-Blende/Wurtzite GaAs Nanowire Heterostructures. *Phys. Rev. B: Condens. Matter Mater. Phys.* **2009**, *80*, 245325.
(31) Parkinson, P.; Joyce, H. J.; Gao, Q.; Tan, H. H.; Zhang, X.; Zou, J.; Jagadish, C.; Herz, L. M.; Johnston, M. B. Carrier Lifetime and Mobility Enhancement in Nearly Defect-Free Core-Shell Nanowires Measured Using Time-Resolved Terahertz Spectroscopy. *Nano Lett.* **2009**, *9*, 3349−3353.
(32) Walukiewicz, W.; Lagowski, J.; Jastrzebski, L.; Gatos, H. C. Minority-Carrier Mobility in P-Type GaAs. *J. Appl. Phys.* **1979**, *50*, 5040−5042.
(33) Perera, S.; Fickenscher, M. A.; Jackson, H. E.; Smith, L. M.; Yarrison-Rice, J. M.; Joyce, H. J.; Gao, Q.; Tan, H. H.; Jagadish, C.; Zhang, X.; Zou, J. Nearly Intrinsic Exciton Lifetimes in Single Twin-Free Gaas/AlGaAs Core-Shell Nanowire Heterostructures. *Appl. Phys. Lett.* **2008**, *93*, 053110.
(34) Gutsche, C.; Niepelt, R.; Gnauck, M.; Lysov, A.; Prost, W.; Ronning, C.; Tegude, F. J. Direct Determination of Minority Carrier Diffusion Lengths at Axial GaAs Nanowire P-N Junctions. *Nano Lett.* **2012**, *12*, 1453−1458.
(35) Lysov, A.; Vinaji, S.; Offer, M.; Gutsche, C.; Regolin, I.; Mertin, W.; Geller, M.; Prost, W.; Bacher, G.; Tegude, F. J. Spatially Resolved Photoelectric Performance of Axial GaAs Nanowire Pn-Diodes. *Nano Res.* **2011**, *4*, 987−995.
(36) Yang, L. J.; Wang, S.; Zeng, Q. S.; Zhang, Z. Y.; Pei, T.; Li, Y.; Peng, L. M. Efficient Photovoltage Multiplication in Carbon Nanotubes. *Nat. Photonics* **2011**, *5*, 673−677.
(37) Hou, J. J.; Han, N.; Wang, F.; Xiu, F.; Yip, S.; Hui, A. T.; Hung, T.; Ho, J. C. Synthesis and Characterizations of Ternary InGaAs Nanowires by a Two-Step Growth Method for High-Performance Electronic Devices. *ACS Nano* **2012**, *6*, 3624−3630.
(38) Heiss, M.; Fontcuberta i Morral, A. Fundamental Limits in the External Quantum Efficiency of Single Nanowire Solar Cells. *Appl. Phys. Lett.* **2011**, *99*, 263102.
(39) Huang, Y.; Duan, X. F.; Wei, Q. Q.; Lieber, C. M. Directed Assembly of One-Dimensional Nanostructures into Functional Networks. *Science* **2001**, *291*, 630−633.
(40) Lee, C. H.; Kim, D. R.; Zheng, X. L. Orientation-Controlled Alignment of Axially Modulated Pn Silicon Nanowires. *Nano Lett.* **2010**, *10*, 5116−5122.
(41) Chae, Y. T.; Kim, J.; Park, H.; Shin, B. Building Energy Performance Evaluation of Building Integrated Photovoltaic (BIPV) Window with Semi-Transparent Solar Cells. *Appl. Energy* **2014**, *129*, 217−227.
(42) Chen, Y. H.; Chen, C. W.; Huang, Z. Y.; Lin, W. C.; Lin, L. Y.; Lin, F.; Wong, K. T.; Lin, H. W. Microcavity-Embedded, Colour-Tuneable, Transparent Organic Solar Cells. *Adv. Mater.* **2014**, *26*, 1129−1134.
(43) Zhang, K.; Qin, C. J.; Yang, X. D.; Islam, A.; Zhang, S. F.; Chen, H.; Han, L. Y. High-Performance, Transparent, Dye-Sensitized Solar Cells for See-Through Photovoltaic Windows. *Adv. Energy Mater.* **2014**, *4*, 1301966.
(44) Colombo, C.; Heiss, M.; Gratzel, M.; Fontcuberta i Morral, A. Gallium Arsenide P-I-N Radial Structures for Photovoltaic Applications. *Appl. Phys. Lett.* **2009**, *94*, 173108.
(45) Wallentin, J.; Anttu, N.; Asoli, D.; Huffman, M.; Aberg, I.; Magnusson, M. H.; Siefer, G.; Fuss-Kailuweit, P.; Dimroth, F.; Witzigmann, B.; Xu, H. Q.; Samuelson, L.; Deppert, K.; Borgstrom, M. T. Inp Nanowire Array Solar Cells Achieving 13.8% Efficiency by Exceeding the Ray Optics Limit. *Science* **2013**, *339*, 1057−1060.
(46) Yoon, J.; Jo, S.; Chun, I. S.; Jung, I.; Kim, H. S.; Meitl, M.; Menard, E.; Li, X. L.; Coleman, J. J.; Paik, U.; Rogers, J. A. Gaas Photovoltaics and Optoelectronics Using Releasable Multilayer Epitaxial Assemblies. *Nature* **2010**, *465*, 329−334.

DOI: 10.1021/acsami.5b06452
ACS Appl. Mater. Interfaces 2015, 7, 20454−20459